

# Number of thermodynamic states in the three-dimensional Edwards-Anderson spin glass

Wenlong Wang,<sup>1</sup> Jonathan Machta,<sup>2,3,\*</sup> Humberto Munoz-Bauza,<sup>1</sup> and Helmut G. Katzgraber<sup>1,3</sup>

<sup>1</sup>*Department of Physics and Astronomy, Texas A&M University, College Station, Texas 77843-4242, USA*

<sup>2</sup>*Department of Physics, University of Massachusetts, Amherst, Massachusetts 01003 USA*

<sup>3</sup>*Santa Fe Institute, 1399 Hyde Park Road, Santa Fe, New Mexico 87501, USA*

The question of the number of thermodynamic states present in the low-temperature phase of the three-dimensional Edwards-Anderson Ising spin glass is addressed by studying spin and link overlap distributions using population annealing Monte Carlo simulations. We consider overlaps between systems with the same boundary condition—which are the usual quantities measured—and also overlaps between systems with different boundary conditions, both for the full systems and also within a smaller window within the system. Our results appear to be fully compatible with a single pair of pure states such as in the droplet/scaling picture. However, our results for whether or not domain walls induced by changing boundary conditions are space filling or not are also compatible with scenarios having many thermodynamic states, such as the chaotic pairs picture and the replica symmetry breaking picture. The differing results for spin overlaps in same and different boundary conditions suggest that finite-size effects are very large for the system sizes currently accessible in low-temperature simulations.

PACS numbers: 75.50.Lk, 75.40.Mg, 05.50.+q, 64.60.-i

## I. INTRODUCTION

The nature of the low-temperature phase of Ising spin glasses is a long-standing mystery and the subject of considerable controversy [1–21]. A central question is whether the low-temperature phase is comprised of a single pair of pure thermodynamic states, or whether the situation is more complicated and involves an infinite number of pure states [22]. For many years, efforts to characterize the low-temperature phase were hampered by confusion over the concept of the thermodynamic limit for systems—such as spin glasses—that may display chaotic size dependence. Chaotic size dependence means that different thermodynamic states may appear in an observation volume in different system sizes or with different boundary conditions. If chaotic size dependence occurs, the usual thermodynamic limit is not meaningful and must be replaced by the so-called *metastate* [23–25], which is a probability distribution over thermodynamic states that may be observed in the observation volumes as the system size changes. Newman and Stein showed that the properties of the metastate are severely constrained for finite-dimensional spin glasses. The metastate may either be trivial and contain a single thermodynamic state consisting of a pair of pure states related by a global spin flip or the metastate may have support on a uncountable infinity of thermodynamic states. The *droplet picture*, developed by McMillan [26], Bray and Moore [27], as well as Fisher and Huse [28–30], is an example of the simple scenario where the metastate consists of a single pair of pure states and the thermodynamic limit may be defined in the usual way. There are two plausible ways that a metastate with support on a continuum of thermodynamic states could occur: Either the *chaotic pairs* [25, 31] scenario where in every finite volume only a single pair of pure states is manifest, or the *nonstandard replica symmetry breaking* (RSB) scenario

[25, 32], where in every volume a countably infinite number of thermodynamic pure states are manifest. The nonstandard RSB scenario is the finite-dimensional analog of Parisi’s replica symmetry breaking solution [22, 33, 34] of the mean-field Sherrington-Kirkpatrick model [35], i.e., the Ising spin glass on the complete graph. The idea that behavior similar to Parisi’s RSB solution of the Sherrington-Kirkpatrick model also applies to the three-dimensional Ising spin glass has a long history [22, 33, 34, 36–39]; the nonstandard RSB scenario being the only mathematically well-defined realization of the mean-field RSB theory in finite dimensions.

One of the key differences between scenarios with many thermodynamic states and a single pair of pure states is whether domain walls induced by changing boundary conditions are space filling. If there is a single thermodynamic state composed of a pair of pure states related by a global spin flip, then the relative domain wall induced by changing from periodic to anti-periodic boundary conditions in a single direction is not space filling. Given an observation window within a much larger system, this domain wall deflects out of the observation window and a single pure state will be seen in the observation volume as the larger volume is taken to infinity. On the other hand, if there is chaotic size dependence and many thermodynamic states, then a change in boundary conditions is likely to induce a completely different thermodynamic state and the relative domain wall will be space filling.

Many numerical studies have attempted to discern which theoretical picture correctly describes short-range systems (see, for example, Refs. [1–21]) resulting in often contradictory conclusions. Most notably, studies of the average distribution of the spin overlap—the order parameter for spin glasses—find a finite weight near zero overlap [5, 6, 9, 12], suggesting a large multiplicity of pure states. However, because finite-size corrections are expected to be severe for currently-available system sizes in simulations, new methods that go beyond simple disorder averaging have been developed to distinguish the different competing pictures [18, 21, 40–42]. These analyses, in contrast, suggest a thermodynamic

---

\*Electronic address: [machta@physics.umass.edu](mailto:machta@physics.umass.edu)

limit with only a single pair of pure states.

To further investigate this problem, in this work we set out to determine whether relative domain walls induced by changing boundary conditions (i.e., overlaps between configurations with different boundary conditions) are space filling and, if not, we measure their fractal dimension directly. To this end, we carry out large-scale Monte Carlo simulations to study the spin and link overlap distributions [9] and measure these overlaps both in a single boundary condition and between spin configurations chosen from different boundary conditions. These measurements are made for both the full volume of the studied system, as well as for an observation window smaller than the full volume. Similar ideas have also been employed in previous work. For example, spin overlap distributions in a small window with the same boundary condition were known to be similar to those in the full system, which has been taken as a support of RSB in Ref. [43]. But when spin overlap functions in a small window between different boundary conditions are studied, this is no longer clear. The spin overlap and link overlap functions between different boundary conditions at zero temperature have also been used in determining whether domain walls are space filling in Refs. [6, 44], however these two studies reach opposite conclusions. Here we revisit this problem systematically at nonzero temperatures. Our results for the spin overlap from differing boundary conditions point toward scenarios having a single thermodynamic state consisting of a pair of pure states (as is the case for the droplet/scaling picture). However, our results for the domain wall induced by changing boundary conditions are also compatible with many pairs of pure states as is the case for the RSB and chaotic pairs picture. We therefore conclude that either accessible system sizes in simulations are still too small despite novel analysis techniques or the nature of the spin-glass state is more complex than expected.

The paper is organized as follows. We first discuss the model, observables and simulation methods in Sec. II, followed by numerical results in Sec. III. Concluding remarks are stated in Sec. IV.

## II. MODEL, OBSERVABLES AND METHODS

We study the three-dimensional Edwards-Anderson (EA) Ising spin-glass model [45] defined by the Hamiltonian

$$H = - \sum_{\langle ij \rangle} J_{ij} S_i S_j, \quad (1)$$

where  $S_i = \pm 1$  are Ising spins and the sum is over nearest neighbors on a cubic lattice of linear size  $L$ . The random couplings  $J_{ij}$  are chosen from a Gaussian distribution with mean 0 and variance 1. A set of couplings  $\mathcal{J} = \{J_{ij}\}$  defines a disorder realization.

We study two primary observables, the spin overlap  $q$  and the link overlap  $q_\ell$  defined, respectively, as

$$q = \frac{1}{\lambda^3} \sum_i S_i^{(1)} S_i^{(2)}, \quad (2)$$

and

$$q_\ell = \frac{1}{dL^3} \sum_{\langle ij \rangle} S_i^{(1)} S_j^{(1)} S_i^{(2)} S_j^{(2)}, \quad (3)$$

where spin configurations “(1)” and “(2)” are chosen independently from the Boltzmann distribution. The sum in Eq. (2) is either over the full lattice with  $L \times L \times L$  sites, or a smaller observation window of size  $W \times W \times W$  with  $W < L$ , and, for these two cases,  $\lambda = L$  and  $\lambda = W$ , respectively. The link overlap is measured only for the full lattice and the sum in Eq. (3) is over nearest neighbors.  $d = 3$  is the space dimension. Two boundary conditions are studied: (i) periodic boundary conditions, referred to as  $\pi$ , and (ii) periodic boundary conditions in the  $y$  and  $z$  directions with anti-periodic boundary conditions in the  $x$  direction, referred to as  $\bar{\pi}$ . The two boundary conditions differ in whether  $S_{\bar{r}+\hat{x}L} = \pm S_{\bar{r}}$  with the  $+$  sign for  $\pi$  and the  $-$  sign for  $\bar{\pi}$ . Averages over the Gibbs distribution are indicated with angular brackets and the boundary condition for the two copies required in the definition of an overlap are specified by subscripts. For example,  $\langle q_\ell \rangle_{\pi, \bar{\pi}}$  is the link overlap between configurations (1) and (2) in boundary conditions  $\pi$  and  $\bar{\pi}$ , respectively. We refer to overlaps between the same boundary condition, either  $(\pi, \pi)$  or  $(\bar{\pi}, \bar{\pi})$ , as *diagonal* overlaps and overlaps between different boundary conditions,  $(\pi, \bar{\pi})$  or  $(\bar{\pi}, \pi)$ , as *off-diagonal* overlaps.

We use population annealing Monte Carlo (PAMC) [46–49] to carry out the simulations. In PAMC, a large population of  $R_0$  replicas of the system, each with the same disorder realization, are annealed in parallel from infinite temperature to a low target temperature,  $T_0 = 1/\beta_0$ . The annealing schedule consists of a sequence of  $N_T$  temperatures equally spaced in inverse temperature  $\beta$ . In a temperature step from  $\beta$  to  $\beta'$  the population is resampled; some members of the population are eliminated and some are reproduced. The mean number of copies of replica  $i$  is proportional to the re-weighting factor,  $\exp[-(\beta' - \beta)E_i]$ . The constant of proportionality is chosen so that the population size remains close to  $R_0$ . Following each resampling step, the population at  $\beta'$  is acted on by  $N_S = 10$  lattice sweeps of the Metropolis algorithm. We simulate  $N_{\text{sa}}$  disorder realizations and measure overlaps at  $T = T_0 = 0.2$  and  $T = 0.42$ . Both of these temperatures are deep in the low-temperature spin-glass phase and should therefore not be affected by critical fluctuations. Overlaps are then measured by pairing independent replicas in the population. The simulation parameters are listed in Table I. A small number of disorder realizations that were not equilibrated using population size listed in Table I were re-run with larger populations until equilibration was achieved.

## III. RESULTS

We discuss the spin overlap in Sec. III A and the link overlap in Sec. III B. When possible, we carry out fits of the data assuming either space filling and non-space filling domain walls and compare the quality of the fits.

TABLE I: Parameters of the simulations for linear system sizes  $L$  and for both periodic ( $\pi$ ) and anti-periodic ( $\bar{\pi}$ ) boundary conditions.  $R_0$  is the population size,  $T_0 = 1/\beta_0$  is the lowest temperature simulated,  $N_T$  the number of temperatures used in the annealing schedule, and  $N_{\text{sa}}$  the number of disorder realizations.

$L$	$R_0$	$1/\beta_0$	$N_T$	$M$
4	$5 \cdot 10^4$	0.200	101	4891
6	$2 \cdot 10^5$	0.200	101	5000
8	$5 \cdot 10^5$	0.200	201	4844
10	$10^6$	0.200	301	4600
12	$10^6$	0.333	301	4137

### A. Spin overlap

The spin overlap distributions  $P_{\mathcal{J}}(q)$  for three typical disorder realizations for the full system ( $L = 8$  and  $T = 0.42$ ) are shown in each of the three panels of Fig. 1. In each panel, the three curves represent the three boundary condition pairs  $(\pi, \pi)$ ,  $(\bar{\pi}, \bar{\pi})$ , and  $(\pi, \bar{\pi})$ . Observe that the two diagonal spin overlaps,  $(\pi, \pi)$  and  $(\bar{\pi}, \bar{\pi})$ , each have peak(s) near the finite-size values of the Edwards-Anderson order parameter,  $\pm q_{\text{EA}}$ . On the other hand, the off-diagonal overlap distributions have peaks that are shifted closer to the origin (i.e.,  $|q| < q_{\text{EA}}$ ) because the domain wall induced by changing boundary conditions reduces the probability of a large value of the spin overlap.

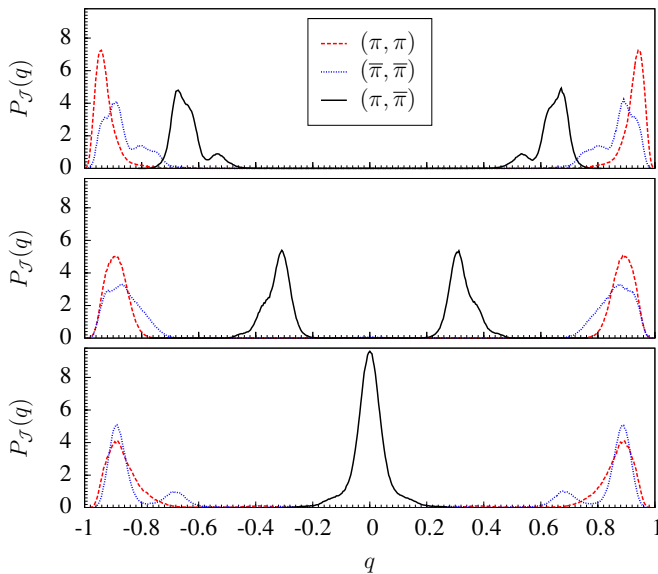


FIG. 1: Spin overlap distributions  $P_{\mathcal{J}}(q)$  for three typical disorder realizations for  $L = 8$  at  $T = 0.42$ . Each panel represents a different disorder realization and, within each panel, the overlap is shown for the boundary condition pairs  $(\pi, \pi)$  (red, dashed),  $(\bar{\pi}, \bar{\pi})$  (blue, dotted) and  $(\pi, \bar{\pi})$  (black, solid). The peaks in  $P_{\mathcal{J}}(q)$  for the off-diagonal pair are shifted away from  $q_{\text{EA}}$  due to the relative domain wall between the periodic and anti-periodic boundary conditions.

Figure 2 shows  $P(q)$ , the disorder averaged spin overlap

distribution for sizes  $L = 4, 6, 8, 10$ , and  $12$  at  $T = 0.42$  for the full lattice. The diagonal overlap distribution displays peaks at finite-size values of  $\pm q_{\text{EA}}$  with  $q_{\text{EA}}$  decreasing with  $L$  while for small  $q$  the distribution is nearly independent of  $L$ , consistent with past studies [5, 9, 12, 18]. The off-diagonal overlap distribution, however, has *no* peaks close to  $\pm q_{\text{EA}}$ . Instead, the curves are nearly independent of  $L$  near  $q = 0$  and seem to approach a relatively flat distribution bounded by  $\pm q_{\text{EA}}$ . It is instructive to compare this with the ferromagnetic Ising model where the domain wall dimension is  $d - 1$ . Because a domain-wall can be inserted anywhere in the system,  $P(q)$  would have a flat distribution between for  $|q| \leq q_{\text{EA}}$ . If a single thermodynamic state picture such as droplet scaling is correct for the EA model, the domain wall is expected to be fractal and the off-diagonal  $P(q)$  has a broad maximum at  $q = 0$  with  $P(q)$  decreasing toward  $\pm q_{\text{EA}}$  just as is seen in Fig. 2. On the other hand, for many state scenarios such as RSB, changing boundary conditions almost always results in a completely different thermodynamic state so that the off-diagonal overlap distribution displays a  $\delta$ -function at the origin in the infinite-volume limit [50]. We see no evidence of a  $\delta$ -function at  $q = 0$ , and the behavior of the off-diagonal spin overlap therefore suggests a single pair of pure states.

To probe the behavior of the off-diagonal spin overlap distribution more quantitatively, we also analyze four statistics of  $P(q)$ :

- $P(0)$ , the value of  $P(q)$  at  $q = 0$ .
- $\langle q^2 \rangle$ , the second moment of  $P(q)$ .
- $I(0.2) = \int_{|q| \leq 0.2} P(q) dq$ .
- $f_q$ , the fraction of disorder realizations having a peak in the overlap distribution centered at  $q = 0$ .

If the relative domain wall is *space filling*, we expect that in the thermodynamic limit

$$\begin{aligned}
 P(0) &\rightarrow \infty, \\
 \langle q^2 \rangle &\rightarrow 0, \\
 I(0.2) &\rightarrow 1, \\
 f_q &\rightarrow 1.
 \end{aligned} \tag{4}$$

However, if the relative domain wall is a *fractal*

$$\begin{aligned}
 P(0) &< \infty, \\
 \langle q^2 \rangle &> 0, \\
 I(0.2) &< 1, \\
 f_q &< 1.
 \end{aligned} \tag{5}$$

Note that disorder averages are implied in the previous equations. The four statistics are shown in Fig. 3. One can see that indeed our data for the off-diagonal overlap distributions are compatible with a fractal relative domain wall and a single pair of pure states, but are not compatible with multiple pure states and space filling domain walls. The fact that the off-diagonal spin overlap suggests a single thermodynamic state

scenario while the diagonal spin overlap suggests a thermodynamic scenario with multiple states implies very large finite-size corrections. This means that the average spin overlap cannot be used in currently accessible simulation system sizes to distinguish between these fundamentally different scenarios.

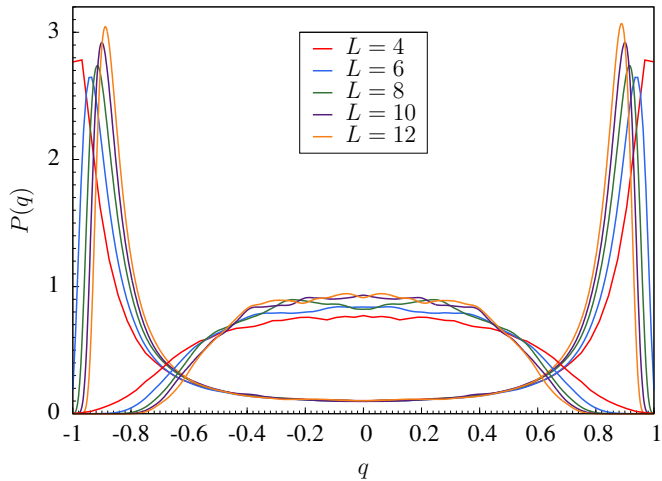


FIG. 2: Disorder-averaged spin overlap distributions  $P(q)$  for the full lattice for sizes  $L = 4, 6, 8, 10,$  and  $12$  at  $T = 0.42$ . The set of curves with peaks at the finite-size value of  $\pm q_{EA}$  and bimodal features correspond to the diagonal overlap distributions while the set of curves with broad maxima at the center correspond to the off-diagonal overlap distributions.

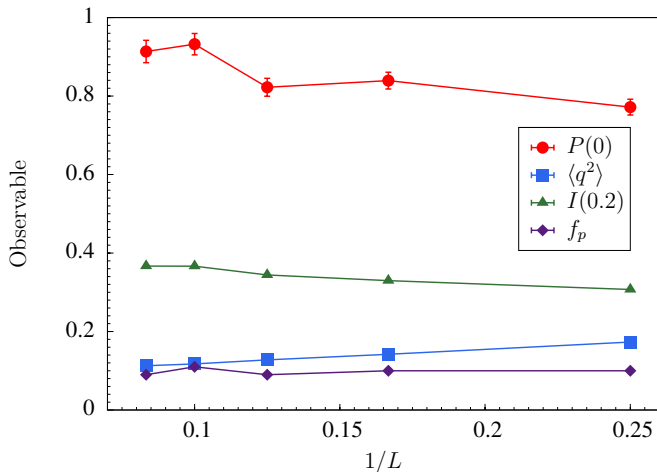


FIG. 3: Four statistics of the off-diagonal overlap distribution:  $P(0)$ ,  $\langle q^2 \rangle$ ,  $I(0.2)$ , and  $f_q$  (see text for details) vs inverse system size  $1/L$ . The expected thermodynamic behavior, i.e.,  $1/L \rightarrow 0$  is described in Eqs. (4) and (5).

We next turn to the behavior of the spin overlap in an observation window of size  $W$  within a system of size  $L \geq W$ . Figure 4 shows spin overlap distributions measured in a window of size  $W = 4$  within a system of size  $L$  with  $L = 4, 6, 8, 10,$  and  $12$  at  $T = 0.42$ . The curves with peaks at  $\pm q_{EA}$  are

the diagonal overlaps. These curves are only slightly dependent on the size of the full system as first noted in Ref. [43]. On the other hand, the off-diagonal spin overlaps do evolve significantly with the size of the full system. It is notable that as  $L$  increases, peaks emerge at the finite-size value of the Edwards-Anderson order parameter. This phenomenon was observed qualitatively for ground states in three dimensions in Ref. [44] and suggests that the domain wall induced by switching boundary conditions might not be space filling and appears to deflect out of the window. If, as  $L$  becomes large, the off-diagonal and diagonal spin overlap become equal, it would be strong evidence in favor of the droplet/scaling picture. However, much larger system sizes would be needed to see such behavior.

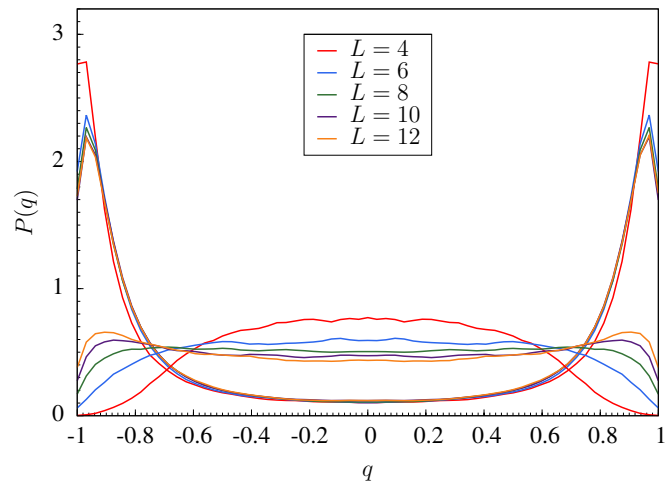


FIG. 4: Disorder-averaged spin overlap distributions  $P(q)$  in a  $W = 4$  observation window within a system of size  $L = 4, 6, 8, 10,$  and  $12$  at  $T = 0.42$ . The sets of curves that display large peaks near  $\pm q_{EA}$ , are the diagonal overlaps. The off-diagonal overlap curves have much smaller weight near  $\pm q_{EA}$ , but that weight increases slowly with the system size  $L$ .

To examine the behavior of the window overlap more quantitatively, we compare integrals of the diagonal and off-diagonal spin overlap peaks in the region near  $\pm q_{EA}$ . We define  $\Gamma_s$  as the difference of the disorder averaged diagonal and off-diagonal overlap distributions measured in the observation window and integrated over a set  $\mathcal{A}$

$$\Gamma_s = \frac{1}{2} \int_{\mathcal{A}} dq [P(q)_{\pi,\pi} + P(q)_{\bar{\pi},\bar{\pi}} - P(q)_{\pi,\bar{\pi}} - P(q)_{\bar{\pi},\pi}]. \quad (6)$$

We set  $\mathcal{A} = [-1, -q_0] \cup (-q_0, 1]$ , where  $q_0$  is chosen to include the  $\pm q_{EA}$  peaks. A similar quantity was studied for ground states in Ref. [44]. If there is indeed a single thermodynamic state and the domain wall deflects out of the window, then  $\Gamma_s$  should approach zero as  $L \rightarrow \infty$ . Furthermore, if the domain wall is a fractal with fractal dimension  $d_s$ , then we expect from box counting that

$$\Gamma_s \sim (L/W)^{d_s-d} \rightarrow 0 \text{ for } L \rightarrow \infty, \quad (7)$$

where  $W$  is the window size,  $d_s$  the fractal dimension of the domain wall, and  $d = 3$  the spatial dimension. A natural cut-off for measuring  $\Gamma_s$  is to set  $q_0 = q_c$ , where  $q_c$  is the crossing point of the off-diagonal spin overlap seen in Fig. 4. For the  $W = 4$  window,  $q_c \approx 0.67$  for  $T = 0.42$  and  $q_c \approx 0.69$  for  $T = 0.2$ . Note, however, that our results are insensitive to the choice of  $q_0$ .

The scaling of  $\Gamma_s$  as a function of  $L$  is shown in Fig. 5. A fit of the form  $\Gamma_s = a(L/W)^{d_s-d}$  yields  $d_s = 2.44(3)$  and  $a = 0.350(6)$  for  $T = 0.42$  and  $d_s = 2.54(3)$  and  $a = 0.378(6)$  for  $T = 0.2$ , with quality of fit [51]  $Q = 0.74$  and  $0.80$ , respectively. Estimates of  $d_s$  are in reasonable agreement with previous results (e.g., Ref. [9]) before extrapolating the aforementioned values to zero temperature. This suggests that the relative domain wall might be deflecting out of the observation window as  $L$  becomes much larger than  $W$ . If the trend continues, this would suggest a fractal domain wall and a single pair of pure states. However, a fit with the assumption of space filling domain walls, i.e.,  $d_s = d$ , of the form

$$\Gamma_s = a + b/(L/W) \rightarrow a \text{ for } L \rightarrow \infty \quad (8)$$

with  $a = 0.103(3)$  and  $b = 0.265(5)$  is of similar quality with  $Q = 0.95$ . The results of both fits at  $T = 0.42$  are shown in Fig. 6. Therefore, the finite-size scaling of  $\Gamma_s$  is not able to distinguish between space-filling and non-space-filling domain walls at these length scales.

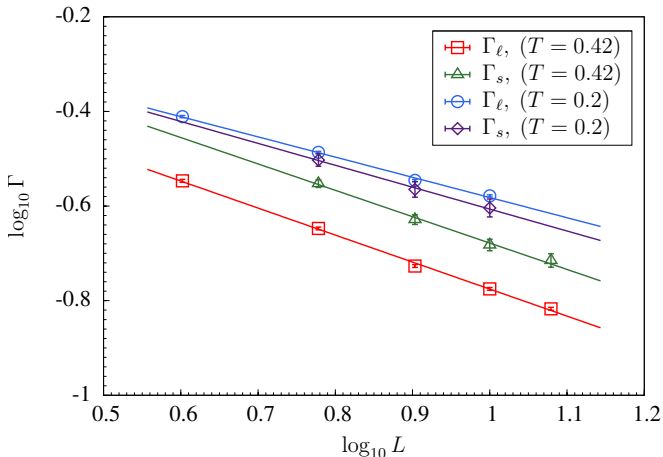


FIG. 5: Scaling of  $\Gamma_s$  (within a window) and  $\Gamma_\ell$  (defined below, for the full systems) as a function of system size  $L$  for  $T = 0.20$  and  $T = 0.42$  together with power law fits (straight lines).

### B. Link overlap

The average link overlap for diagonal and off-diagonal pairs of boundary conditions for the full system are shown in Fig. 7. In agreement with many previous studies, e.g., Ref. [9], the average diagonal link overlap is nearly independent of system size. On the other hand, the average off-diagonal link overlap

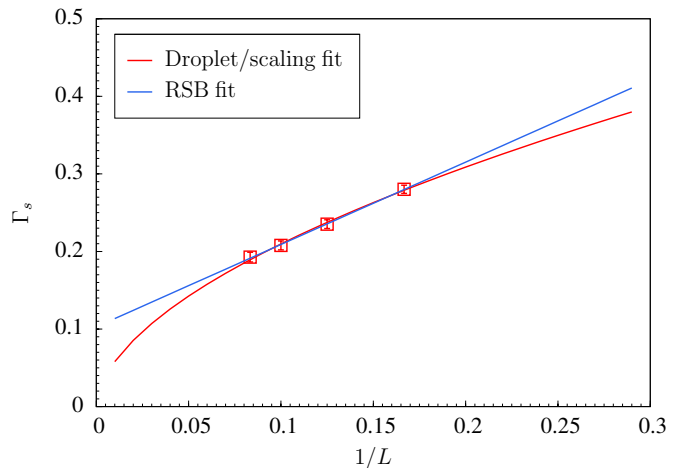


FIG. 6: Comparison of the fits of  $\Gamma_s$  assuming droplet/scaling (red curved line, power law) or a RSB (blue straight line, constant and finite-size correction) at  $T = 0.42$ . Both functional forms fit the data comparably well, i.e.,  $\Gamma_s$  does not distinguish the two pictures at these length scales. See text for details of fits.

is an increasing function of system size. If there is a single thermodynamic state and the relative domain wall induced by the change of boundary conditions is not space filling, then the diagonal and off-diagonal link overlap distribution should become identical in the large volume limit. To test this hypothesis, we consider the difference between diagonal and off-diagonal link overlaps,

$$\Gamma_\ell = [\langle \langle q_\ell \rangle_{\pi, \pi} + \langle q_\ell \rangle_{\bar{\pi}, \bar{\pi}} - \langle q_\ell \rangle_{\pi, \bar{\pi}} - \langle q_\ell \rangle_{\bar{\pi}, \pi}] / 2, \quad (9)$$

where the double brackets indicates a disorder average. The difference between the diagonal and off-diagonal link overlaps is the average volume occupied by the relative domain wall induced by changing boundary conditions. Thus, if this domain wall has fractal dimension  $d_s$  and we compute  $\Gamma_\ell$  in a system of size  $L$ , we again expect by box counting

$$\Gamma_\ell \sim L^{d_s-d}. \quad (10)$$

Figure 5 shows a log-log plot of  $\Gamma_\ell$  as a function of  $L$  and, from a power law fit, we estimate  $d_s = 2.43(1)$  at  $T = 0.42$  and  $d_s = 2.57(2)$  at  $T = 0.2$  with quality of fit of  $Q = 0.098$  and  $0.017$ , respectively. These values (including the temperature dependence) are in agreement with the results of Ref. [52]. Furthermore, the results at the lower temperature are in reasonable agreement with the zero-temperature estimates of Refs. [5] and [9].

However, fits with  $\Gamma_\ell \rightarrow a > 0$ , implying space filling domain walls (i.e.,  $d_s = d$ ) and multiple thermodynamic states are similarly satisfactory. For  $T = 0.2$ , a fit of the form  $\Gamma_\ell = a + b/L + c/L^2$  yields  $a = 0.15(2)$ ,  $b = 1.2(3)$  and  $c = 1.0(7)$  with  $Q = 0.03$ . The uncertainty in  $c$  is very large because of the shape of the error ellipse of the three-parameter fit, but it should be noted that a two-parameter fit with  $c$  set to zero is of much lower quality although it has a similar value of  $a$ . This RSB fit is shown in Fig. 8 along with the two-parameter power

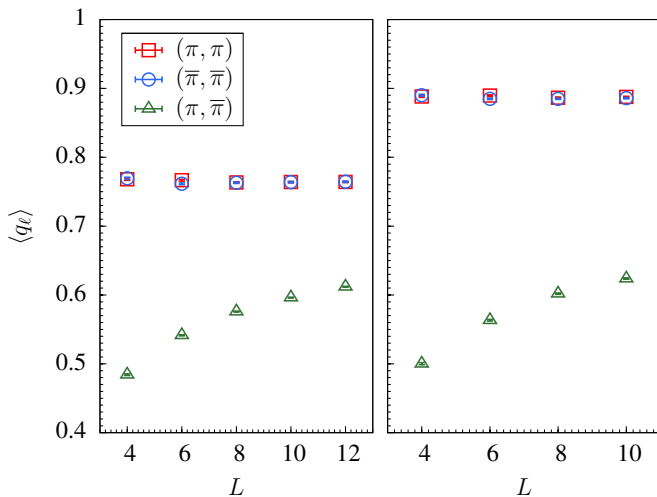


FIG. 7: Average of the link overlap  $\langle q_\ell \rangle$  as a function of system size  $L$  for the three pairs of boundary conditions and temperatures  $T = 0.42$  (left panel) and  $T = 0.2$  (right panel). Note that as  $L$  increases the off-diagonal link overlap increases toward the diagonal link overlap.

law fit  $\Gamma_\ell = aL^{(d_s-3)}$  with  $a = 0.7(2)$  and  $d_s = 2.57(2)$  with  $Q = 0.017$ . Neither fit is high quality and  $\Gamma_\ell$  cannot distinguish the two scenarios at these length scales.

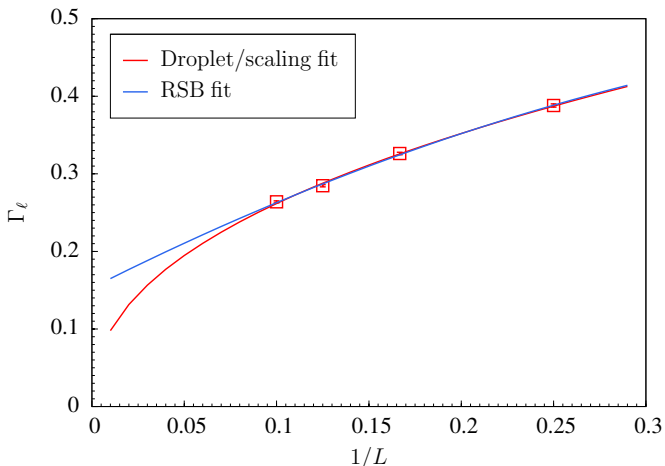


FIG. 8: Comparison of the fits of  $\Gamma_\ell$  assuming droplet/scaling (red curve, power law) or a RSB (blue darker curve, constant and finite-size corrections) at  $T = 0.2$ . Both functional forms fit the data comparably well, i.e.,  $\Gamma_\ell$  does not distinguish the two pictures at these length scales. See text for details of fits.

#### IV. SUMMARY AND FUTURE CHALLENGES

We have investigated the spin and link overlaps between the same and different boundary conditions for the full system as well as in a smaller observation window in the three-

dimensional Edwards-Anderson Ising spin glass. We find that the *off-diagonal* spin overlap function for the full system is relatively flat and nearly independent of system size, in agreement with a single thermodynamic state consisting of a pair of pure states. This metric not used to date represents another way to differentiate different theoretical scenarios.

On the other hand, as has been noted in previous studies, the *diagonal* spin overlap function is nonzero and nearly independent of systems size near  $q = 0$ , which supports scenarios with many thermodynamic states. The two sets of results together imply that for system sizes currently accessible to low-temperature simulations, the average spin overlap is incapable of distinguishing the two scenarios for the three-dimensional Edwards-Anderson model. A detailed analysis of the link overlap and the spin overlap in a window is consistent with fractal domain walls that have a fractal dimension near  $d_s \approx 2.5$ . However, we cannot rule out space filling domain walls.

While the use of  $1/L$  finite-size corrections is reasonable for the studied system sizes and hence we cannot rule out space-filling domain walls, we believe it is an important future challenge to find a theoretical basis for the used scaling form. In contrast, the ground-state energy per spin  $e$  has corrections that scale as  $e = a+b/L^x$ , where  $x = d-\theta \approx 2.76$  in three dimensions [53]. This exponent is much larger, and using such a large exponent, the space-filling fits for our data are no longer satisfactory. While it is possible that different quantities may show different finite-size corrections at the zero-temperature fixed point, it is still important to find a theoretical basis to explain why the  $1/L$  corrections are needed when studying the scaling of the link overlap, yet not for the ground-state energy per spin.

Substantially larger system sizes would be required to clearly determine whether domain walls induced by changing boundary conditions are space filling or not using average spin overlaps in windows or link overlaps. Since the first large-scale simulations in 2001 approximately 15 years have passed. Betting on Moore's Law [54] we expected to be able to revisit this problem and bring more clarity into the different theoretical descriptions of the spin-glass state. However, our results clearly show that more effort needs to be put into the development of better algorithms, as well as new statistics to tackle these problems.

#### Acknowledgments

W.W., H.M.B and H.G.K. acknowledge support from the National Science Foundation (Grant No. DMR-1151387). J.M. acknowledges support from the National Science Foundation (Grant No. DMR-1507506). We would like to thank E. Marinari, M. A. Moore, G. Parisi, and D. Stein for comments and discussions. H.G.K. thanks Paul Hobbs for providing multiple sources of inspiration. The work of H.G.K., H.M.B., and W.W. is supported in part by the Office of the Director of National Intelligence (ODNI), Intelligence Advanced Research Projects Activity (IARPA), via MIT Lincoln Laboratory Air Force Contract No. FA8721-05-C-0002. The

views and conclusions contained herein are those of the authors and should not be interpreted as necessarily representing the official policies or endorsements, either expressed or implied, of ODNI, IARPA, or the U.S. Government. The

U.S. Government is authorized to reproduce and distribute reprints for Governmental purpose notwithstanding any copyright annotation thereon. We thank Texas A&M University for access to their Ada and Curie clusters.

- 
- [1] M. Mézard, G. Parisi, N. Sourlas, G. Toulouse, and M. Virasoro, *Nature of the Spin-Glass Phase*, Phys. Rev. Lett. **52**, 1156 (1984).
- [2] M. A. Moore, H. Bokil, and B. Drossel, *Evidence for the droplet picture of spin glasses*, Phys. Rev. Lett. **81**, 4252 (1998).
- [3] B. Drossel, H. Bokil, M. A. Moore, and A. J. Bray, *The link overlap and finite size effects for the 3d Ising spin glass*, Euro. Phys. J. **13**, 369 (2000).
- [4] F. Krzakala and O. C. Martin, *Spin and link overlaps in 3-dimensional spin glasses*, Phys. Rev. Lett. **85**, 3013 (2000).
- [5] M. Palassini and A. P. Young, *Nature of the spin glass state*, Phys. Rev. Lett. **85**, 3017 (2000).
- [6] E. Marinari and G. Parisi, *On the effects of changing the boundary conditions on the ground state of Ising spin glasses*, Phys. Rev. B **62**, 11677 (2000).
- [7] E. Marinari, G. Parisi, F. Ricci-Tersenghi, J. J. Ruiz-Lorenzo, and F. Zuliani, *Replica symmetry breaking in short range spin glasses: A review of the theoretical foundations and of the numerical evidence*, J. Stat. Phys. **98**, 973 (2000).
- [8] E. Marinari, G. Parisi, F. Ricci-Tersenghi, and J. J. Ruiz-Lorenzo, J. Phys. A **33**, 2373 (2000).
- [9] H. G. Katzgraber, M. Palassini, and A. P. Young, *Monte Carlo simulations of spin glasses at low temperatures*, Phys. Rev. B **63**, 184422 (2001).
- [10] A. A. Middleton, *Energetics and geometry of excitations in random systems*, Phys. Rev. B **63**, 060202(R) (2001).
- [11] N. Hatano and J. E. Gubernatis, *Evidence for the droplet picture in the 3d  $\pm J$  spin glass*, Phys. Rev. B **66**, 054437 (2002).
- [12] H. G. Katzgraber and A. P. Young, *Monte Carlo simulations of spin-glasses at low temperatures: Effects of free boundary conditions*, Phys. Rev. B **65**, 214402 (2002).
- [13] H. G. Katzgraber and A. P. Young, *Monte Carlo studies of the one-dimensional Ising spin glass with power-law interactions*, Phys. Rev. B **67**, 134410 (2003).
- [14] H. G. Katzgraber and A. P. Young, *Geometry of large-scale low-energy excitations in the one-dimensional Ising spin glass with power-law interactions*, Phys. Rev. B **68**, 224408 (2003).
- [15] G. Hed and E. Domany, *Nontrivial link overlap distribution in three-dimensional Ising spin glasses*, Phys. Rev. B **76**, 132408 (2007).
- [16] L. Leuzzi, G. Parisi, F. Ricci-Tersenghi, and J. J. Ruiz-Lorenzo, *Diluted One-Dimensional Spin Glasses with Power Law Decaying Interactions*, Phys. Rev. Lett. **101**, 107203 (2008).
- [17] R. Alvarez Baños, A. Cruz, L. A. Fernandez, J. M. Gil-Narvion, A. Gordillo-Guerrero, M. Guidetti, A. Maiorano, F. Mantovani, E. Marinari, V. Martin-Mayor, et al., *Nature of the spin-glass phase at experimental length scales*, J. Stat. Mech. P06026 (2010).
- [18] B. Yucesoy, H. G. Katzgraber, and J. Machta, *Evidence of Non-Mean-Field-Like Low-Temperature Behavior in the Edwards-Anderson Spin-Glass Model*, Phys. Rev. Lett. **109**, 177204 (2012).
- [19] A. Billoire, L. A. Fernandez, A. Maiorano, E. Marinari, V. Martin-Mayor, G. Parisi, F. Ricci-Tersenghi, J. J. Ruiz-Lorenzo, and D. Yllanes, *Comment on "Evidence of Non-Mean-Field-Like Low-Temperature Behavior in the Edwards-Anderson Spin-Glass Model"*, Phys. Rev. Lett. **110**, 219701 (2013).
- [20] B. Yucesoy, H. G. Katzgraber, and J. Machta, *Yucesoy, Katzgraber, and Machta reply*, Phys. Rev. Lett. **110**, 219702 (2013).
- [21] W. Wang, J. Machta, and H. G. Katzgraber, *Evidence against a mean-field description of short-range spin glasses revealed through thermal boundary conditions*, Phys. Rev. B **90**, 184412 (2014).
- [22] G. Parisi, *Infinite number of order parameters for spin-glasses*, Phys. Rev. Lett. **43**, 1754 (1979).
- [23] M. Aizenman and J. Wehr, *Rounding effects of quenched randomness on first-order phase transitions*, Comm. Math. Phys. **130**, 489 (1990).
- [24] C. M. Newman and D. L. Stein, *Spatial Inhomogeneity and Thermodynamic Chaos*, Phys. Rev. Lett. **76**, 4821 (1996).
- [25] C. M. Newman and D. L. Stein, *Metastate approach to thermodynamic chaos*, Phys. Rev. E **55**, 5194 (1997).
- [26] W. L. McMillan, *Domain-wall renormalization-group study of the two-dimensional random Ising model*, Phys. Rev. B **29**, 4026 (1984).
- [27] A. J. Bray and M. A. Moore, *Scaling theory of the ordered phase of spin glasses*, in *Heidelberg Colloquium on Glassy Dynamics and Optimization*, edited by L. Van Hemmen and I. Morgenstern (Springer, New York, 1986), p. 121.
- [28] D. S. Fisher and D. A. Huse, *Ordered phase of short-range Ising spin-glasses*, Phys. Rev. Lett. **56**, 1601 (1986).
- [29] D. S. Fisher and D. A. Huse, *Absence of many states in realistic spin glasses*, J. Phys. A **20**, L1005 (1987).
- [30] D. S. Fisher and D. A. Huse, *Equilibrium behavior of the spin-glass ordered phase*, Phys. Rev. B **38**, 386 (1988).
- [31] C. M. Newman and D. L. Stein, *Multiple states and thermodynamic limits in short-ranged Ising spin-glass models*, Phys. Rev. B **46**, 973 (1992).
- [32] N. Read, *Short-range Ising spin glasses: the metastate interpretation of replica symmetry breaking*, Phys. Rev. E **90**, 032142 (2014).
- [33] G. Parisi, *The order parameter for spin glasses: a function on the interval 0–1*, J. Phys. A **13**, 1101 (1980).
- [34] G. Parisi, *Order parameter for spin-glasses*, Phys. Rev. Lett. **50**, 1946 (1983).
- [35] D. Sherrington and S. Kirkpatrick, *Solvable model of a spin glass*, Phys. Rev. Lett. **35**, 1792 (1975).
- [36] R. Rammal, G. Toulouse, and M. A. Virasoro, *Ultrametricity for physicists*, Rev. Mod. Phys. **58**, 765 (1986).
- [37] M. Mézard, G. Parisi, and M. A. Virasoro, *Spin Glass Theory and Beyond* (World Scientific, Singapore, 1987).
- [38] A. P. Young, ed., *Spin Glasses and Random Fields* (World Scientific, Singapore, 1998).
- [39] G. Parisi, *Some considerations of finite dimensional spin glasses*, J. Phys. A **41**, 324002 (2008).
- [40] A. A. Middleton, *Extracting thermodynamic behavior of spin glasses from the overlap function*, Phys. Rev. B **87**, 220201 (2013).
- [41] C. Monthus and T. Garel, *Typical versus averaged overlap dis-*

- tribution in spin glasses: Evidence for droplet scaling theory*, Phys. Rev. B **88**, 134204 (2013).
- [42] M. Wittmann, B. Yucesoy, H. G. Katzgraber, J. Machta, and A. P. Young, *Low-temperature behavior of the statistics of the overlap distribution in Ising spin-glass models*, Phys. Rev. B **90**, 134419 (2014).
- [43] E. Marinari, G. Parisi, F. Ricci-Tersenghi, and J. J. Ruiz-Lorenzo, *Small window overlaps are effective probes of replica symmetry breaking in three-dimensional spin glasses*, J. Phys. A: Mathematical and General **31**, L481 (1998).
- [44] M. Palassini and A. P. Young, *Triviality of the ground state structure in Ising spin glasses*, Phys. Rev. Lett. **83**, 5126 (1999).
- [45] S. F. Edwards and P. W. Anderson, *Theory of spin glasses*, J. Phys. F: Met. Phys. **5**, 965 (1975).
- [46] K. Hukushima and Y. Iba, in *The Monte Carlo method in the physical sciences: celebrating the 50th anniversary of the Metropolis algorithm*, edited by J. E. Gubernatis (AIP, 2003), vol. 690, p. 200.
- [47] E. Zhou and X. Chen, in *Proceedings of the 2010 Winter Simulation Conference (WSC)* (Springer, Baltimore MD, 2010), p. 1211.
- [48] J. Machta, *Population annealing with weighted averages: A Monte Carlo method for rough free-energy landscapes*, Phys. Rev. E **82**, 026704 (2010).
- [49] W. Wang, J. Machta, and H. G. Katzgraber, *Population annealing: Theory and application in spin glasses*, Phys. Rev. E **92**, 063307 (2015).
- [50] T. Aspelmeier, W. Wang, M. A. Moore, and H. G. Katzgraber, *Interface free-energy exponent in the one-dimensional Ising spin glass with long-range interactions in both the droplet and broken replica symmetry regions*, Phys. Rev. E **94**, 022116 (2016).
- [51] W. H. Press, S. A. Teukolsky, W. T. Vetterling, and B. P. Flannery, *Numerical Recipes in C* (Cambridge University Press, Cambridge, England, 1995).
- [52] W. Wang, J. Machta, and H. G. Katzgraber, *Chaos in spin glasses revealed through thermal boundary conditions*, Phys. Rev. B **92**, 094410 (2015).
- [53] S. Boettcher and S. Falkner, *Finite-size corrections for ground states of Edwards-Anderson spin glasses*, Eur. Phys. Lett. **98**, 47005 (2012).
- [54] G. Moore, *Cramming more components onto integrated circuits*, Electronics Magazine **38**, 114 (1965).